Korean J. Chem. Eng., 39(4), 1045-1052 (2022)
DOI: 10.1007/s11814-021-0945-7

pISSN: 0256-1115
eISSN: 1975-7220

Integrating advanced Keggin-structure polyoxometalate into polymeric membrane to enhance photocatalytic self-cleaning and antifouling functionalities

Daniel Chin Hao Koo*, Nee Nee Tan*, Qi Hwa Ng*,,†, Siti Kartini Enche Ab Rahim*,**,†, Siew Chun Low***, and Ryan Yow Zhong Yeo***

*Faculty of Chemical Engineering Technology, Universiti Malaysia Perlis (UniMAP), Perlis, Malaysia
**Frontier Materials Research, Centre of Excellence (FrontMate), Universiti Malaysia Perlis (UniMAP), Perlis, Malaysia
***School of Chemical Engineering, Engineering Campus, Universiti Sains Malaysia,
Seri Ampangan, 14300 Nibong Tebal, S.P.S., Penang, Malaysia
(*Received 23 June 2021 • Revised 27 August 2021 • Accepted 30 August 2021*)

Abstract−The high photocatalytic activity of environmentally benign Keggin-type polyoxometalate (POM) was introduced into polyethersulfone (PES) membrane to promote membrane anti-fouling and self-cleaning functionality. Neat PES and POM/PES hybrid membranes were synthesized via phase inversion method. X-ray diffraction (XRD) and attenuated total reflection-Fourier transform infrared (ATR-FTIR) spectroscopy proved the success of synthesizing Keggin-type POM. The traits of the membranes were evaluated using scanning electron microscopy (SEM), ATR-FTIR, contact angle measurement, porosity and porometer. The hydrophilicity of all the POM/PES hybrid membranes was enhanced and resulted in the reduction of contact angle of the membrane (52.21 ± 0.1101^{o}, 45.11 ± 0.6657^{o} and 50.30 ± 0.1054^{o}) for 0.025, 0.05 and 0.1 wt% POM/PES hybrid membranes, respectively, compared to that of the neat PES membrane (57.30 ± 0.0817^{o}). Additionally, all the POM/PES hybrid membranes showed excellent anti-fouling and self-cleaning characteristics as compared to that of the neat PES membrane. 0.05 wt% POM/PES hybrid membrane outstood all the other membranes, which marks the HA rejection at 77.12% and was able to achieve flux recovery ratio (FRR) of 111.34% with temporal superhydrophilicity effect in just merely 150 seconds at 254 nm UV irradiation.

Keywords: Keggin-type Polyoxometalate, Hybrid Membrane, Self-cleaning, Water Filtration, High Efficiency Photodegradation

INTRODUCTION

All sorts of living organisms and, eventually, the natural environment rely on water. It is truly undeniable that all the living things could not survive without water. However, water quality has deteriorated over time as the evidence shows the escalating level of various toxic organic and inorganic compounds in both ground and surface water [1], including some sources of natural organic matter (NOM) which is made up of humic acid (HA). Indeed, HA is the precursor of trihalomethane (THM), a carcinogenic compound produced in the process of chlorination and disinfection of drinking water [2]. Therefore, the removal of HA from water body has caught much attention for its environmental and health concern.

Membrane technology is indeed great for removing aquatic HA, but HA deposition on it causes membrane fouling, a major challenge that restricts its application [3]. Membrane fouling can reduce permeate flux across the membrane, increase operating pressure, and reduce the lifespan of the membrane [4], consequently incurring higher operating and replacement cost of membrane. Nevertheless, hybrid membranes (e.g., TiO_2/PES hybrid membrane, graphene oxide (GO)/PES hybrid membrane, and ZrO_2/PES hybrid membrane) appear to be a solution with higher fouling resistance, higher flux across membrane and higher retention of pollutants [5-7]. In short, from recent researches, it is incontestable that the performance of hybrid membrane will significantly be improved as compared to the neat membrane.

Polyoxometalate (POM) is a class of versatile and discrete anionic metal oxides in the Group 5 and 6 in the periodic table, which contain unique chemical and physical properties [8]. POM has attracted much attention for its diverse molecular structures, unique redox properties and a strong oxidant, which has potential in oxidizing most organic compounds to carbon dioxide and water under irradiation of UV light [9]. In this approach, Keggin-type POM was introduced into PES membrane to provide the self-cleaning function to the membrane, which is to photodegrade the foulants accumulated on the hybrid membrane surface via UV light emission. Through this membrane self-cleaning method, flux recovery of fouled hybrid membrane is anticipated. In fact, the mass of POM added in the membrane reveals the degree of photocatalytic activity, which acts to degrade the attached foulants on the membrane surface. Hence, the efficiency of the extent of photocatalytic activity due to different amounts of POM added in the membrane was investigated in the current study through its flux recovering ability.

MATERIALS AND METHODS

1. Chemicals and Materials

All chemicals were used as obtained without further modification

†To whom correspondence should be addressed.
E-mail: qhng@unimap.edu.my, sitikartini@unimap.edu.my

or purification. Sodium tungstate dihydrate ($Na_2WO_4 \cdot 2H_2O$) and *p*-Nitrophenyl phosphate, disodium salt, hexahydrate ($C_6H_4NO_6P \cdot 2Na \cdot 6H_2O$) were purchased from Merck (Darmstadt, Hessen, Germany), which are the raw chemicals used to synthesize POM. Sulfuric acid (H_2SO_4) received from Fisher Scientific International (Hampton, New Hampshire, USA) was used to adjust the pH of POM solution. Ethanol (C_2H_6O) obtained from VWR International (Radnor, Pennsylvania, USA) was used to purify the POM synthesized. To synthesize the membrane, the Ultrason E6020P PES polymer with MW of 58 kDa was supplied by BASF (Ludwigshafen, Germany), while the solvent used to dissolve the polymer, N-methyl-2-pyrrolidone (NMP) was purchased from Merck (Darmstadt, Hessen, Germany). In the current research, HA obtained from Sigma-Aldrich (St. Louis, MO, USA) was used as the organic foulant to study the membrane performance and fouling test via the crossflow filtration system. 1 M of hydrochloric acid (HCl) and 1 M of sodium hydroxide (NaOH) supplied by Merck (Darmstadt, Hessen, Germany) were prepared for the HA pH adjustment.

2. Synthesis of Keggin-type POM Photocatalyst

15 mL of deionized (DI) water was added to 5 g of $Na_2WO_4 \cdot 2H_2O$ and the mixture was stirred continuously until all $Na_2WO_4 \cdot 2H_2O$ was dissolved. Then, 0.3 g of $C_6H_4NO_6P \cdot 2Na \cdot 6H_2O$ was added into the mixture. After dissolving $C_6H_4NO_6P \cdot 2Na \cdot 6H_2O$, the pH of the mixture was adjusted to pH ca. 1-2 using H_2SO_4. A light green precipitate was formed. The reaction mixture was kept in a dark place for a day. Then, the precipitate was rinsed with DI water and dried at 100 °C to remove water. Ethyl alcohol was added to further purify the precipitate and remove through heating process at 80 °C. Rinsing and drying process with DI water was repeated to obtain the final product of darkish green POM.

The synthesized POM was qualitatively characterized using XRD (Bruker D2 Phaser, Billerica, Massachusetts, USA), equipped with a copper (Cu) X-ray tube at 10 mA and 30 kV. The wavelength, $K_{\alpha 1}$, used was at 1.5406 Å. 1 g of POM was filled densely into the 25 mm diameter shallow well of the sample holder. The powder surface was prepared in a flat smooth way to minimize the orientation preferred and to achieve high quality and precise XRD result. Meanwhile, ATR-FTIR (PerkinElmer Inc., Waltham, Massachusetts, USA) was used to identify the chemical composition of POM synthesized. Data was collected for 32 seconds within wavelength of 600 to 4,000 nm.

3. Membrane Preparation

First, the moisture of the PES polymer was removed using an oven at 40 °C. Next, a 13 wt% of PES polymer solution was prepared by the addition of PES polymer into the N-methyl-2-pyrrolidone (NMP) solvent. The mixture was instantaneously sealed with parafilm which was subjected to 70 °C for 60 minutes and followed by room temperature for 4 hours with a constant stirring of 500 rpm. Subsequently, the POM synthesized was added into the prepared polymer solution with 0 (neat PES membrane), 0.025, 0.05 and 0.1 wt% of POM under intensive sonication, forming the POM/PES solution. A 200 μm thickness of the mixture was then cast onto a flat glass plate and was immediately dipped into a distilled water coagulation bath for a day. This was to complete the wet phase-inversion process and to remove the residual solvent. The synthesized neat PES membrane and POM/PES hybrid membranes were kept in a zipper bag containing DI water before performing characterization and membrane filtration performance test.

For membrane characterization, SEM (Hitachi TM3000, Japan) was used to observe the surface morphology of the synthesized membranes. The samples were coated with a thin layer of platinum (Pt) to provide electrical conductivity and avoid the samples from being burnt, using a sputter coater (Quorum Technologies Ltd, Laughton, East Sussex, UK). The mean pore size distribution of the synthesized membranes was determined using a capillary flow porometer, Porolux 1000 (Benelux Scientific, Belgium). Meanwhile, 1 cm×1 cm of synthesized membrane samples were prepared for membrane porosity measurement. The initial weight of the membrane sample was noted as W_1. The samples were then put in the oven and dried at 40 °C for 20 minutes. Subsequently, the weight of the membrane samples was measured and recorded as W_2. The drying and weighing procedure were repeated until the reading of W_2 reached constant. The porosity of the membrane in percentage was then calculated using Eq. (1):

$$P = \left(\frac{v_a - v_e}{v_a}\right) \times 100\% \quad (1)$$

where P is the membrane porosity (%), v_a is the apparent volume (cm^3) and v_e is the existence volume (cm^3).

The static contact angle measurement of the synthesized membrane was also carried out using sessile drops (Rame-Hart, USA). A known water droplet volume was dropped on top of the membrane via the automated micro-syringe dispenser. The shape of the water dispensed on the membrane surface was recorded by a high-speed framing camera. Young's equation was applied to determine the contact angle of the membrane surface. ATR-FTIR (PerkinElmer Inc., Waltham, Massachusetts, USA) was used to identify the chemical composition of the synthesized membrane. Data was collected within 32 seconds with the wavelength of 600 to 4,000 nm.

4. Membrane Crossflow Filtration and Self-cleaning Evaluation

Crossflow filtration system was used to evaluate the membrane performance, as depicted in Fig. 1, with an effective membrane area of 4.1 cm^2. Pressure in the filtration system was generated by the booster pump and controlled by the needle valves. Prior filtration process, membrane was compressed in the crossflow filtration system for 30 minutes at 1.5 bar, to compact the pores for stable pure water flux. Constant pressure of 10 psi was used, while the flowrate was controlled at 250 mL/min. The pure water flux (J_{w_o}) for both neat PES and POM/PES hybrid membranes was measured as a function of time at a constant pressure of 10 psi until a quasi-steady flux was achieved, which typically was within 30 minutes.

Then, the filtration process was repeated at a constant pressure of 10 psi by replacing with 20 mg/L of HA. The data collected was used to evaluate the filtration flux (J_1) for up to 2 hours of filtration time. After obtaining the constant flux, the membrane was rinsed by circulating pure water to remove the loosely bound HA. The pure water flux was also recorded. The membrane along with the cell was then removed from the filtration system to place in a black box containing a pen-ray photochemical quartz lamp (90-0049-06 UVP, German) with 254 nm wavelength as UV light source. The distance of the UV lamp and the membrane was fixed to 5 cm,

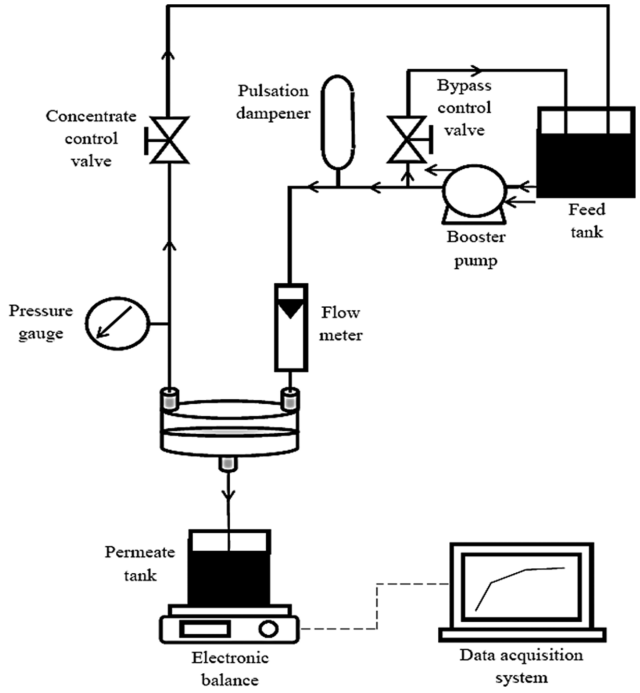

Fig. 1. Schematic diagram of the crossflow filtration system.

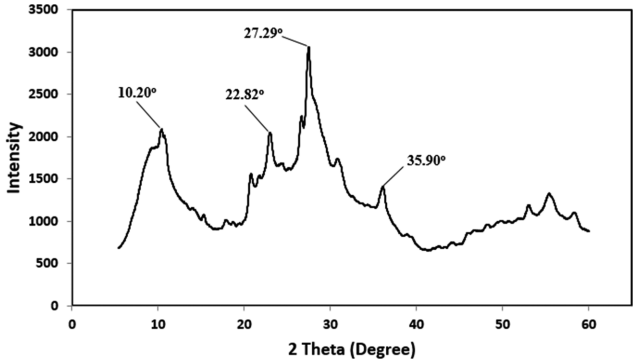

Fig. 2. XRD pattern for the Keggin-type POM photocatalyst.

and set for 150 seconds of photodegradation. After the photodegradation process, the membrane was then rinsed again by re-circulating pure water to remove the UV degraded HA using the crossflow filtration system. The pure water flux was recorded. All the steps were repeated to get the error bar and standard deviation. The flux profiles were recorded and the flux recovery ratio (FRR) was determined based on Eq. (2):

$$\mathrm{FRR}=\frac{J_{w_1}}{J_{w_o}}\times 100\% \tag{2}$$

where FRR is the flux recovery ratio (%), J_{w_1} is the pure water flux at any predetermined time (L/m^{2}hr) and cleaning condition, while J_{w_o} is the initial pure water flux (L/m^{2}hr).

To obtain the HA rejection percentage (R) of the given membranes, the permeate concentration of HA was determined at the end of every crossflow filtration via ultraviolet-visible (UV-Vis) spectrophotometer (UV 1800 Shimadzu, Japan) with wavelength of 254 nm. Eq. (3) was used to calculate the rejection percentage (R) of the given membranes:

$$\mathrm{R}=\left(1-\frac{C_P}{C_F}\right)\times 100\% \tag{3}$$

where R is the rejection percentage (%), C_P is the permeate concentration (mg/L) and C_F is the feed concentration (mg/L).

RESULTS AND DISCUSSION

1. Incorporation of Keggin-type POM in PES Membrane

The synthesized POM was first qualitatively characterized using XRD, with diffraction spectrum plotted as in Fig. 2. The four significant intensities of 2θ emerging in the XRD diffractogram were 10.20°, 22.82°, 27.29° and 35.90°, respectively. These peaks lay within or very close to the 2θ with ranges of 7° to 10°, 16° to 23°, 25° to 30° and 31° to 38° that validated the synthesized POM photocata-

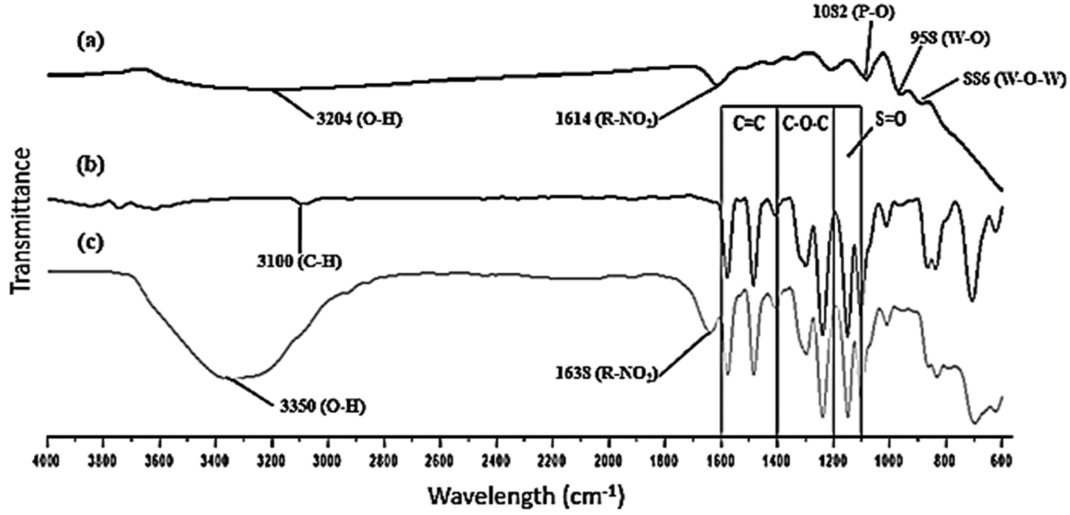

Fig. 3. ATR-FTIR spectra of (a) Keggin-type POM photocatalyst, (b) neat PES membrane and (c) POM/PES hybrid membranes.

lyst is Keggin-type [10,11]. It is imperative to verify the Keggin-type structure of POM because only Keggin structure of POM possesses good photocatalytic activity and stability [12,13], which resists structure changes under the process of multielectron redox [14]. Henceforth, with high potential in oxidizing most of the organic compounds such as humic acid to carbon dioxide and water.

Additionally, the synthesized POM was further characterized via ATR-FTIR, as shown in Fig. 3(a), where peak wavelengths of 886, 958, 1,082 and 3,204 cm^{-1} were observed. The peak at 3,204 cm^{-1} indicates the presence of O-H groups on the POM surface, which is in good agreement with numerous reports [15,16]. Major features of Keggin structure can be identified in the peaks of 886, 958 and 1,082 cm^{-1}, which are attributed to the vibrations of W-O-W, W-O and P-O, respectively [10,17]. According to El-Naggar and co-researchers [17], the P-O bond is identified as the PO_4^{3-} tetrahedral vibration. As a result, the basic geometry and structure of Keggin anion can be confirmed with these three peaks observed. The combination of XRD and ATR-FTIR results has proven that Keggin-type POM was synthesized successfully.

Neat PES membrane, 0.025, 0.05 and 0.1 wt% POM/PES hybrid membranes were cast via phase inversion method. Top view of all the membranes was observed using SEM (Fig. 4). In terms of the membrane physical morphologies, there is no considerable difference between the pore size and porosity of the membranes, with or without the presence of POM in PES. Nevertheless, a more obvious crystal structure and higher amount of POM was observed (Fig. 4(d)) on the membrane surface with higher dosage of POM in casting dope.

To further prove that the POM/PES hybrid membranes were synthesized successfully, the synthesized membrane was characterized via ATR-FTIR. Fig. 3(b) shows the spectrum of neat PES membrane. The characteristic of the peaks matches with the chemical structure of the PES which consists of sulfone structure, ether bond and benzene ring. Peaks observed at 1,110 and 1,156 cm^{-1} are attributed to the stretching of S=O due to the sulfone structure of PES. Meanwhile, peaks at 1,244 and 1,304 cm^{-1} can be attributed to the stretching of C-O-C ether bond. The vibration of the benzene aromatic skeletal causes three peaks at 1,414, 1,490 and 1,584 cm^{-1}. The C-H stretching of the benzene ring is identified at 3,100 cm^{-1}. All the peaks situated in Fig. 3(b) were well-supported by Qu and co-researchers [18].

Comparison was made between Fig. 3(b) and Fig. 3(c) to identify the difference between the neat PES and POM/PES hybrid membranes. Their absorption peaks are very similar, with the traces of the S=O stretching, C-O-C stretching and C=C. However, the peak for C-H stretching is not detected in Fig. 3(c). This might be due to the addition of hydrophilic POM in PES to cause the increment of the hydroxyl group. Consequently, greatly improving the

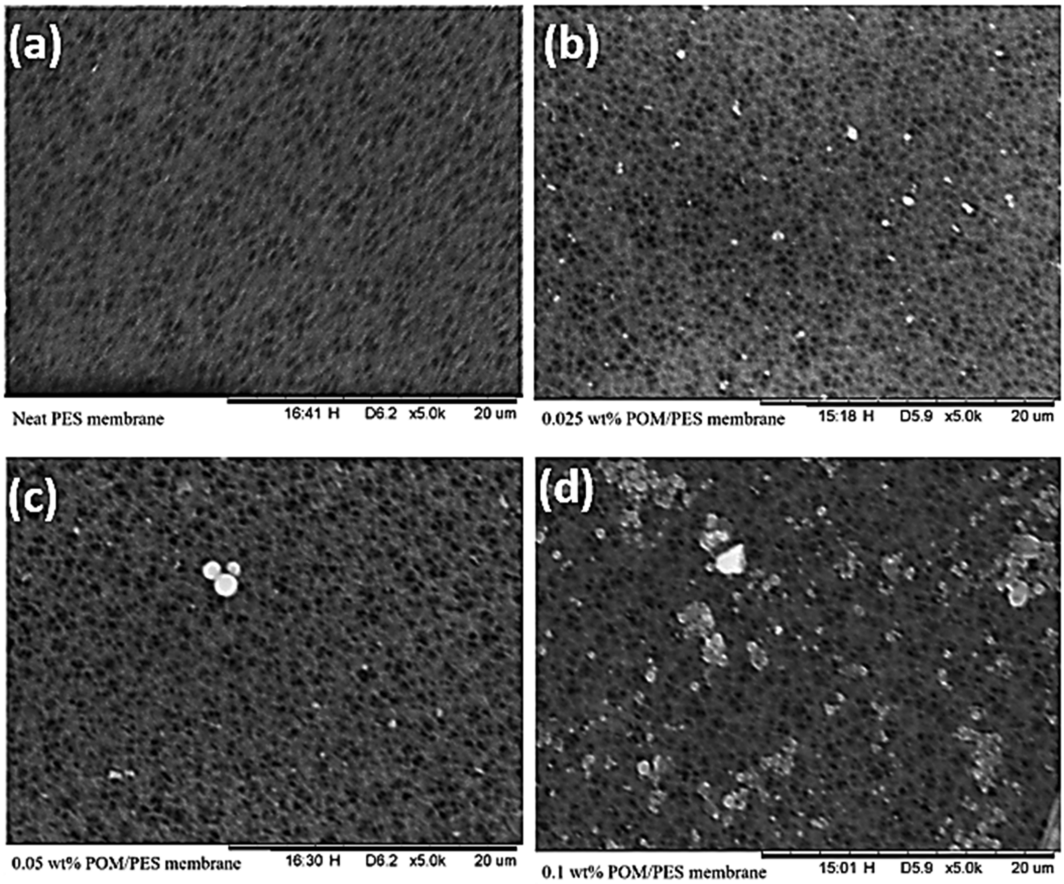

Fig. 4. SEM top surface morphology images of (a) neat PES membrane, (b) 0.025 wt%, (c) 0.05 wt% and (d) 0.1 wt% POM/PES hybrid membranes, respectively. Scanning was done at 15 kV with 5000× magnification.

Table 1. Mean pore size distribution and porosity of the ultrafiltration membrane synthesized

Membrane	Mean pore size distribution (μm)	Porosity
Neat PES	0.1104	0.8513±0.0103
0.025 wt% POM/PES	0.0546	0.8553±0.0390
0.05 wt% POM/PES	0.0737	0.8765±0.0218
0.1 wt% POM/PES	0.0584	0.7734±0.0604

broad peak intensity at 3,350 cm^{-1} which has probably masked the C-H stretching peak of weaker intensity. Meanwhile, two obvious absorption peaks that emerged were also observed at 1,638 and 3,350 cm^{-1}, as depicted in Fig. 3(c). The peak of 1,638 cm^{-1} is associated with the aromatic ring vibration (RNO_2) origin from the POM. The appearance of aromatic ring vibration (RNO_2) proves the presence of POM in POM/PES hybrid membrane. The infrared band at 3,350 cm^{-1} is attributed to the bending and stretching of a hydroxyl group (O-H) on the surface of POM/PES hybrid membrane [15,16]. This is most probably due to the higher affinity of POM towards water molecules and the hydrophilic character possessed by POM as a tiny particle [19-21]. Indeed, the presence of the hydroxyl group on the POM/PES hybrid membrane surface could increase the photocatalytic activity. The hydroxyl group will interact with the photogenerated holes, which leads to superior charge transfer and restrains the electron-hole pairs from recombining [22]. These two absorption peaks proved the successful synthesis of POM/PES hybrid membrane.

Table 1 summarizes the porosity and mean pore size distribution of membranes. The mean pore sizes of all membranes were less than 1 μm, which indicates the ultrafiltration characteristic of the membrane [23]. Neat PES membrane has the highest mean pore size distribution, 0.1104 μm, while the hybrid membranes have demonstrated smaller mean pore distribution, varying from 0.0546 to 0.0737 μm. Such observation is because of the introduction of POM in the hybrid membranes. As reported in another study regarding TiO_2/PSF membrane, the mean pore radius of the membranes was reduced, ranging from 8.9 to 9.3 nm with 1 to 2 wt% TiO_2, as compared to the neat PSF membrane, with 10.6 nm mean pore radius [24].

Based on Table 1, the porosity of the neat PES was the least, 0.8513±0.0103 as compared to 0.025 and 0.05 wt% POM/PES with porosity of 0.8553±0.0390 and 0.8765±0.0218, respectively. This was due to the presence of the hydrophilic tiny particles in the polymer solution, as POM would escalate the solvent and non-solvent exchange rate during immersion precipitation, which indirectly increases the membrane porosity [25]. Whereas, among all the synthesized membrane, the smallest porosity was dominated by the 0.1 wt% POM/PES hybrid membrane with a value of 0.7734±0.0604. The further adding of POM to the membrane will not enhance the porosity, but the porosity will drop drastically to lower than the neat PES membrane. The sudden reduction in the porosity can be accounted by the blocking of the pores of the membrane by the POM tiny particles during the phase inversion process [21].

In fact, one of the utmost crucial characteristics of membrane is the surface hydrophilicity that accounts for its anti-fouling and flux of the membrane [24]. Generally, membrane with contact angle less than 90° would have better adhesiveness, wettability and high solid surface free energy than that of contact angle higher than 90° [20]. Therefore, the reduction of contact angle of a membrane means that the membrane is more hydrophilic. In this current work, the contact angle values for neat PES membrane, 0.025, 0.05 and 0.1 wt% POM/PES hybrid membranes, were 57.30±0.0817°, 52.21±0.1101°, 45.11±0.6657° and 50.30±0.1054°, respectively. Among all the membranes tested, the neat PES membrane had the greatest water droplet contact angle, reflecting its relatively hydrophobic character than POM/PES hybrid membranes.

In contrast, by adding POM, the values of contact angle of POM/PES hybrid membranes were reduced. This is due to the higher affinity of POM towards water molecules and the hydrophilic character possessed by POM as a nanoparticle [19-21]. Contact angle was decreased from 52.21° to 45.11° when higher amount of POM was added, from 0.025 to 0.05 wt%. However, an increment of contact angle to 50.30° was detected when further increasing the amount of POM to 0.1 wt%. This occurrence might be clarified as the increasing concentration of POM that facilitates a higher tendency of POM to agglomerate as evidenced by SEM image (Fig. 4(d)). These agglomerations in turn result in the reduction in their exposed specific surface area that could be interacting with water molecules on the membrane surface, which indirectly leads to the increase of the contact angle [26].

2. Anti-fouling Ability of Membrane

The effect of POM dosage in PES hybrid membrane with HA rejection is depicted in Fig. 5. As shown, HA rejection was increased to 77.12% with the increase of POM dosage from 0 to 0.05 wt%. This is because of the hydrophilicity properties of membrane earlier and the emerging smaller mean pore size of the membrane (Table 1), which contributes to an optimistic effect to the rejection of HA. Unfortunately, severe decrease in the retention of HA to only 66.34% was observed once the concentration of POM had increased to 0.1 wt%. As earlier shown in Fig. 4(d), POM/PES hybrid membranes with higher POM photocatalyst concentration contained a more noticeable crystal structure of the POM photocatalyst on the membrane top surface. Thus, it produced a rougher surface as compared to that of other synthesized membranes. Membrane top surface with higher roughness certainly results in more fouling [27-29].

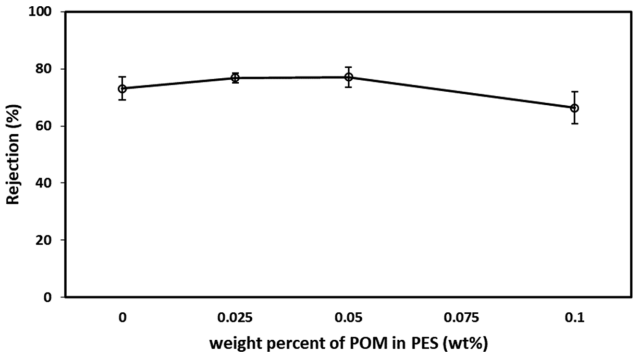

Fig. 5. Function of POM dosage in PES with HA rejection.

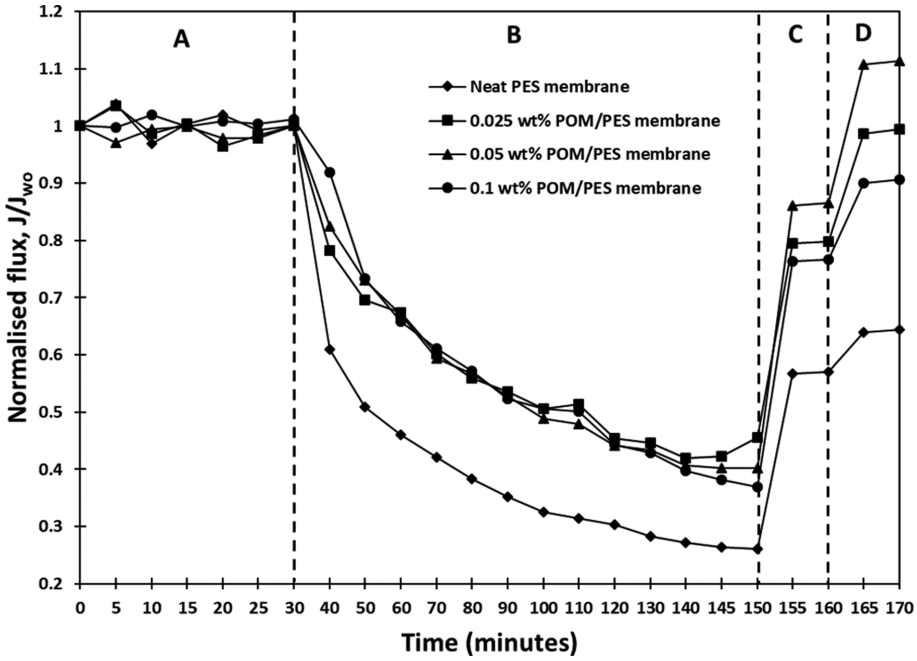

Fig. 6. Graph of normalized flux of membrane against time (Region A: Feed with DI water to allow the membrane to reach quasi-equilibrium steady state; Region B: HA filtration process; Region C: Membrane cleaning process (DI water); Region D: Membrane cleaning process (UV irradiation plus water cleaning)).

Fig. 6 illustrates the anti-fouling and self-cleaning properties of the membrane synthesized in a normalized graph against time. For the first 30 minutes (region A, Fig. 6), similar fluxes were observed with insignificant differences. As in region A (Fig. 6), the feed was just deionized (DI) water to allow the membrane to reach quasi-equilibrium steady state.

After 30 minutes (region B, Fig. 6), the feed was replaced by HA solution for filtration process until 150 minutes. The neat PES membrane showed a drastic drop among all the membranes prepared. This means the neat PES membrane was easily fouled as compared to the POM/PES hybrid membranes. The greater hydrophilicity property of the POM/PES hybrid membranes was less susceptible to HA fouling by adhering water molecules on the top of membrane surface [30]. Therefore, an interfacial hydration layer would form on the membrane surface and beneficially reduce the chances of adsorption of organic substances (HA in the current study) onto the membrane [16,30]. This undeniably enhanced the anti-fouling property of the PES membrane. Moreover, in the agreement of the larger mean pore size distribution of the neat PES membrane, HA particles would get trapped within the interior structure of the membranes, which brings the plugging effect of pores. The entrapped HA particles account for the extra resistance against the flowing path of permeates passing though the membranes and cause the flux to be lowered over time.

It is interesting that at exactly 150 minutes, the last point in region B (Fig. 6), the 0.1 wt% POM/PES hybrid membrane marks the lowest normalized flux as compared to that of the 0.025 and 0.05 wt% POM/PES hybrid membranes. This can be related back to the increase in surface roughness of the 0.1 wt% POM/PES hybrid membrane, which is due to the addition of crystal structure appearance of POM photocatalyst (Fig. 4(d)). The increment in surface roughness will allow higher adsorption of foulant onto the membrane surface, leading to flux decline [27]. Thus, the surface roughness of the membrane is said to be directly correlated to the fouling.

After 150 minutes (region C, Fig. 6), membrane cleaning with deionized water was carried out for ten minutes to physically remove any reversible foulant. Later, the membranes were illuminated to the UV source for 150 seconds and sent back for another 10 minutes of washing using deionized water to remove the irreversible foulant, as demonstrated in region D (Fig. 6). Based on Fig. 6 (region C), the permeate fluxes of all membranes managed to recover to a certain extent with just the physical water cleaning. The FRR of the neat PES membrane was just 57.09%, which is generally the lowest as compared to the POM/PES hybrid membranes. As discussed earlier, the contact angle for POM/PES hybrid membranes was generally lower than the neat PES membrane, which indicated a better property in hydrophilicity. This caused relatively weaker interaction between HA foulant and POM/PES hybrid membrane, hence inflicting more reversible fouling than irreversible fouling. POM/PES hybrid membranes were able to recover the fluxes easier by just the physical water cleaning than the neat PES membrane. However, irregular trend of FRR for POM/PES hybrid membranes was observed after the physical water cleaning (region C, Fig. 6). The FRR was 79.86%, 86.60% and 76.70% for 0.025, 0.05 and 0.1 wt% POM in PES membrane, respectively. Such trend is in good agreement with that of the contact angle results. Due to high hydrophilicity properties of the 0.05 wt% POM/PES membrane, it showed the most outstanding result, which recovers up to about 86.60% of its initial water flux.

After the UV irradiation plus water cleaning (region D, Fig. 6),

the FRR values were raised to an even greater extent. This effect should not be applicable to neat PES membrane as it does not contain POM. However, the less notable increase in FRR for neat PES membrane is probably due to the creation of pressure differences during the cycles of water cleaning. Based on Fig. 6 (region D), all the POM/PES hybrid membrane had outstood the neat PES membrane in terms of FRR. This means the self-cleaning function and anti-fouling property of the photocatalytic membrane via UV emission had been established. The enhancement is justified by the photocatalytic property of POM, which generates strong oxidant reagents such as hydroxyl and superoxide radicals. These oxidizing agents mineralize most of the organic pollutants that accumulate on the membrane surface regardless of selectivity and the process is very quick. In this study, 0.05 wt% of hybrid POM/PES membrane achieved up to 111.34% of FRR with only 150 seconds duration of UV irradiation.

In contrast, the 0.1 wt%, POM/PES hybrid membrane only attained 90.59% of flux recovery rate under the same period of UV irradiation. This is because the 0.05 wt% POM/PES hybrid membrane contained well-distributed POM on the membrane surface (Fig. 4(c)), while POM aggregate was found on the surface of the 0.1 wt% POM/PES hybrid membrane (Fig. 4(d)). It is unquestionable that the lower total surface area of the photocatalyst results in lower photocatalytic activity [31]. Therefore, the performance of 0.05 wt% POM/PES hybrid membrane was better than that of 0.1 wt%.

Indeed, the addition of POM photocatalyst in the PES membrane requires a lower UV irradiation time, with merely just 150 seconds to obtain high or nearly perfect flux recovery. By comparing similar membrane treatment researches through UV emission, durations used to clean the membranes with UV ranged from 60 to 600 minutes to achieve approximately 100% of flux recovery ratio. The summary of the current and other researchers' work is tabulated in Table 2. In this work, the time required for UV irradiation to achieve a high flux recovery rate is significantly less than that repeatedly by the other researchers. This is due to the contribution of the lower band gap energy of POM photocatalyst [32] and the presence of huge amount of hydroxyl group, in conjunction with the obvious appearance of peak 3,356 cm^{-1} in Fig. 3(c). These traits boost the photocatalytic activity of the membranes greatly by allowing electrons in the narrow and valence bands to be excited more easily in the presence of UV light [15]. In the meantime, the addition of POM photocatalyst improves the hydrophilicity of the hybrid membranes. The enhancement of both of the characteristics further enhances the self-cleaning property of POM/PES hybrid membrane as the hydrophilicity and photocatalysis effects occur simultaneously on the membrane surface [33]. Consequently, with the aid of UV light illumination, organic pollutants such as humic acid can be degraded and washed away effortlessly via water circulation.

CONCLUSION

POM/PES hybrid membrane was synthesized successfully. The peaks obtained from ATR-FTIR and SEM images were able to distinguish neat PES and POM/PES hybrid membranes. Additionally, the POM/PES hybrid membrane was further characterized using contact angle measurement, porometer and porosity. Based on the characterization, in a general view, it has been proven that the POM/PES hybrid membrane has better membrane traits such as lower contact angle, smaller membrane pores and high voidage. For the study in different POM concentration, 0.05 wt% POM/PES hybrid membrane surpasses all the other membranes, mark at 77.12% of HA rejection. Although the anti-fouling property of the hybrid membranes was similar, the anti-fouling property was significantly improved as compared to the neat PES membrane. The other obvious augmentation was the self-cleaning feature of 0.05 wt% hybrid membrane which achieved a flux recovery ratio of 111.34% with merely just UV irradiation time of 2.5 minutes. The flux recovery ratio established higher than 100% was accounted for the temporal superhydrophilicity effect. Overall, findings in this study have revealed the potential of the hybrid membrane to be a noble and breakthrough technology for a safer, better, and more stable drinking water supply.

ACKNOWLEDGEMENTS

The author would like to acknowledge the support from the Fundamental Research Grant Scheme (FRGS) under a grant number of FRGS/1/2021/TK0/UNIMAP/02/3 from the Ministry of Higher Education Malaysia. Furthermore, sincere indebtedness and gratitude is addressed to Universiti Malaysia Perlis (UniMAP).

Table 2. Summary of this study and recent works by other researchers

Membrane	Photocatalyst concentration (wt%)	Cleaning time (min)	Flux recovery (%)	Type of organic pollutants	Reference
POM/PES	0.05	2.5	111	HA	Current work
POM/PES	0.1	2.5	91	HA	Current work
TiO_2/PVDF	3	60	102	BSA	[23]
TiO_2/PVDF	6	60	112	BSA	[23]
K-B-N-tripledoped TiO_2/PES	0.5	60	100	Palm oil mill effluent	[34]
TiO_2-PEG/PVDF	1.5	480	90	HA	[35]
TiO_2/Al_2O_3	-	600	95	Acid orange 7	[33]
B-TiO_2-SiO_2-CoF_2O_4/PES	0.1	60	99	Powder milk solution	[15]
TiO_2-PEG/PVDF	1.5	90	70	HA	[25]

REFERENCES

1. A. Ayati, M. N. Shahrak, B. Tanhaei and M. Sillanpää, *Chemosphere*, **160**, 30 (2016).
2. R. K. Padhi, S. Subramanian, A. K. Mohanty and K. K. Satpathy, *J. Water Process Eng.*, **29**, 100769 (2019).
3. S. Javdaneh, M. R. Mehrnia and M. Homayoonfal, *Korean J. Chem. Eng.*, **32**, 1 (2016).
4. Y. Yang, S. Qiao, R. Jin, J. Zhou and X. Quan, *Korean J. Chem. Eng.*, **35**, 964 (2018).
5. X. Li, X. Fang, R. Pang, J. Li, X. Sun, J. Shen, W. Han and L. Wang, *J. Membr. Sci.*, **467**, 226 (2014).
6. S. Zinadini, A. A. Zinatizadeh, M. Rahimi, V. Vatanpour and H. Zangeneh, *J. Membr. Sci.*, **453**, 292 (2014).
7. R. Pang, X. Li, J. Li, Z. Lu, X. Sun and L. Wang, *Desalination*, **332**, 60 (2014).
8. S. Omwoma, C. T. Gore, Y. Ji, C. Hu and Y.-F. Song, *Coord. Chem. Rev.*, **286**, 17 (2015).
9. C. G. Liu, T. Zheng, S. Liu and H. Y. Zhang, *J. Mol. Struct.*, **1110**, 44 (2016).
10. A. Aouissi, S. S. Al-Deyab, A. Al-Owais and A. Al-Amro, *Int. J. Mol. Sci.*, **11**, 2770 (2010).
11. L. E. Briand, H. J. Thomas and G. T. Baronetti, *Appl. Catal. A*, **201**, 191 (2000).
12. S. Liu, Y. Liu, S. Jiang, S. Liu, D. He, N. Li, J. Miao and J. Ye, *J. Environ. Chem. Eng.*, **4**, 908 (2016).
13. Z. Zhang, H. Ma, H. Pang, C. Zhang, D. Chai and Y. Hou, *J. Solid State Chem.*, **258**, 170 (2018).
14. S. Sampurnam, S. Muthamizh, T. Dhanasekaran, D. Latha, A. Padmanaban, P. Selvam, A. Stephen and V. Narayanan, *J. Photochem. Photobiol. A*, **370**, 26 (2019).
15. H. Zangeneh, A. A. Zinatizadeh, S. Zinadini, M. Feyzi and D. W. Bahnemann, *Sep. Purif. Technol.*, **209**, 764 (2019).
16. X. Zhao, H. Xuan, Y. Chen and C. He, *J. Membr. Sci.*, **494**, 48 (2015).
17. M. R. El-Naggar, R. F. Aglan and M. S. Sayed, *J. Environ. Chem. Eng.*, **1**, 516 (2013).
18. P. Qu, H. Tang, Y. Gao, L. Zhang and S. Wang, *Bioresources*, **5**, 2323 (2010).
19. J. Garcia-Ivars, M.-I. Iborra-Clar, M.-I. Alcaina-Miranda, J.-A. Mendoza-Roca and L. Pastor-Alcañiz, *Chem. Eng. J.*, **283**, 231 (2016).
20. T. D. Kusworo and D. P. Utomo, *J. Environ. Chem. Eng.*, **5**, 6077 (2017).
21. T. Djoko, N. Ariyanti and D. Puji, *J. Water Process Eng.*, **35**, 101190 (2020).
22. K. Ahmad Fuad and S. K. Enche Ab Rahim, *Int. J. Curr. Res. Sci. Eng. Technol.*, **1**, 300 (2018).
23. J.-P. Méricq, J. Mendret, S. Brosillon and C. Faur, *Chem. Eng. Sci.*, **123**, 283 (2015).
24. Y. Yang, H. Zhang, P. Wang, Q. Zheng and J. Li, *J. Membr. Sci.*, **288**, 231 (2007).
25. H. Younas, H. Bai, J. Shao, Q. Han, Y. Ling and Y. He, *J. Membr. Sci.*, **541**, 529 (2017).
26. A. M. Munshi, V. N. Singh, M. Kumar and J. P. Singh, *J. Appl. Phys.*, **103**, 084315 (2008).
27. C. Hobbs, J. Taylor and S. Hong, *J. Water Supply Res. T.*, **55**, 559 (2006).
28. M. N. Subramaniam, P. S. Goh, E. Sevgili, M. Karaman, W. J. Lau and A. F. Ismail, *Eur. Polym. J.*, **122**, 109360 (2020).
29. E. M. V Hoek, S. Bhattacharjee and M. Elimelech, *Langmuir*, **19**, 4836 (2003).
30. M. Fathizadeh, W. L. Xu, F. Zhou, Y. Yoon and M. Yu, *Adv. Mater. Interfaces*, **1600918**, 1 (2017).
31. G. Fang, J. Liu, X. Yan, D. Wang, J. Israr and T. Xue, *Adv. Mater. Interfaces*, **1800844**, 1 (2018).
32. F. Clavería-Cádiz, R. Arratia-Pérez and D. MacLeod-Carey, *Polyhedron*, **117**, 478 (2016).
33. J. Mendret, M. Hatat-Fraile, M. Rivallin and S. Brosillon, *Sep. Purif. Technol.*, **111**, 9 (2013).
34. H. Zangeneh, A. A. Zinatizadeh, S. Zinadini, M. Feyzi and D. W. Bahnemann, *React. Funct. Polym.*, **127**, 139 (2018).
35. H. Song, J. Shao, Y. He, B. Liu and X. Zhong, *J. Membr. Sci.*, **405-406**, 48 (2012).